Multidimensional Governing Equations of Matrix Flow Component of Subsurface Stormflow as Function of Bedrock Surface Geometry

M. Levent Kavvas[1,2], Tongbi Tu[3,*], Ali Ercan[2] and Z.Q. Chen[4]

[1]Hydrologic Research Laboratory, Department of Civil and Environmental Engineering, University of California, Davis, CA 95616, USA.

[2]J. Amorocho Hydraulics Laboratory (JAHL), Department of Civil and Environmental Engineering, University of California - Davis, CA, 95616, USA

[3]School of Civil Engineering, Sun Yat-sen University, Guangzhou, 510275, China

[4] California Department of Water Resources, Sacramento, California

*Correspondence to: Tongbi Tu (tutb@mail.sysu.edu.cn)

ABSTRACT

Various field studies have shown the fundamental influence of the bedrock surface geometry on subsurface stormflow (SSSF). Various field studies have also shown that the SSSF process consist of at least two major components: the matrix flow component and the macropore flow component that are in dynamic interaction toward forming the SSSF. This study focuses on the matrix flow component of SSSF. Furthermore, field studies have shown that the bedrock surface that underlies the SSSF has essentially a two-dimensional (2D) geometry, where not only the longitudinal profile along the hillslope but also the transverse profile perpendicular to the main hillslope direction influence the subsurface stormflow over the bedrock. The macropore flow itself being a multidimensional flow process, the general setting for the dynamic interaction of the matrix flow and macropore flow components of SSSF is the treatment of both of these processes as multidimensional flow processes. Within this framework, this study attempts to extend the existing 2D Boussinesq model for the matrix flow over an inclined flat 2D surface in the longitudinal hillslope direction by developing the governing equations of matrix flow at hillslope scale over various 2D bedrock surface geometries that are reported in the field studies of SSSF. Then a numerical experiment is performed by applying the developed governing equations to two different bedrock surface geometries. The results of the numerical simulations of the matrix flow component of SSSF show the impact of the 2D bedrock surface geometry on the characteristics of the matrix flow in both longitudinal and transvers directions over a hillslope.

Keywords: Matrix flow; Subsurface stormflow; bedrock surface geometry; hillslope; governing equations.

1. INTRODUCTION

Due to various field studies of subsurface flow at hillslopes of a watershed during 1960s and 1970s (e.g., Whipkey, 1965; Hewlett and Hibbert, 1967; Ragan, 1968; Weyman, 1973; Dunne and Black, 1970, 1971), culminating in the seminal work of Dunne (1978), subsurface stormflow (SSSF) was established as a fundamental component of watershed runoff. In the ensuing four decades many valuable field studies were performed around the world to develop a better understanding of the flow mechanisms that constitute SSSF and to understand various physical factors that determine the characteristics of SSSF (e.g. Mosley, 1979; Jones, 1981, 2010; McDonnell et al. 1990, 1996; Tsuboyama et al. 1994; Sidle et al. 1995, 2000, 2001; Woods and Rowe, 1996; Tani, 1997; Noguchi et al. 1997, 1999; Freer et al. 2002; Uchida et al. 2002; Weiler and McDonnell, 2006; Kosugi et al. 2006; Uchida and Asano, 2010; Mueller et al. 2014; McKnight et al. 2015; Martini et al. 2015; Guo et al. 2019). From a study of this literature and of the reviews of field and modeling studies of SSSF (e.g. Weiler et al. 2005; Beven and Germann, 2013; Chifflard et al. 2010), one can draw some inferences on the basic characteristics of SSSF at the hillslopes of a watershed: a) SSSF takes place mainly over an impeding (infiltrating) bedrock surface in the forms of both matrix flow as well as channelized macropore flow (Sidle et al. 1995, 2000, 2001; Noguchi et al. 1999); b) however, besides the above two main flow processes, fracture flows within the bedrock may contribute significantly to the total SSSF by interacting both with macropore and matrix flows over the surface of the bedrock (Noguchi et al. 1999; Weiler et al. 2005; Guo et al. 2019); c) the bedrock surface geometry plays a fundamental role in determining the location, peak flow and flow volumes of SSSF (Freer et al. 2002); d) drainable porosity varies with soil depth (Weiler et al. 2005). Based on these inferences it is necessary to develop viable models of matrix flow, macropore flow and bedrock fracture flow processes at hillslope and watershed scales while accounting for their dynamic interactions at the hillslope scale. In developing viable models for matrix flow and macropore flow processes, it is also necessary to account for the effect the bedrock surface geometry exerts on these processes.

Valuable attempts were made to model both matrix flows and macropore flows as individual flow processes as well as their dynamic interactions. Since the focus of this study is modeling matrix flows, in the following only the literature on modeling matrix flows and their interactions with macropore flows is reviewed. For modeling matrix flow the multidimensional 2D (two dimensional) or 3D unsaturated-saturated Darcy-Richards equations (e.g. Freeze 1972a,b; Sloan and Moore, 1984; Loague et al. 2006; Keim et al. 2006; Tromp-van Meerveld, 2004; Nieber and Sidle 2010), 1D hydraulic-head-based Boussinesq equations (Boussinesq, 1877; Henderson and Wooding, 1964; Childs, 1971; Brutsaert, 2005), 2D hydraulic-head-based Boussinesq equations (Kavvas et al. 2004; Chen et al. 2004a; Brutsaert, 2005), 1D storage-type Boussinesq equations (Troch et al. 2003; Hilberts et al. 2004; Troch et al. 2013), 1D storage type Kinematic wave approximations to Boussinesq equations (Sloan and Moore, 1984; Fan and Bras, 1998; Troch et al. 2002), and hydraulic head-based kinematic wave approximation (Beven 1981) were used. Models of the dynamic interaction of matrix flows with macropore flows are reviewed in Simunek et al. (2003), Gerke (2006), Kohne et al. (2009) and Beven and Germann (2013). For modeling the dynamic interaction of matrix flows with macropore flows mainly the multidimensional Darcy-Richards equations for the presentation of the matrix flow component were employed. One type of such models are dual-porosity models where the matrix water is generally considered immobile and the matrix can only store water or exchange water with the soil macropores/preferential pathways (Phillip, 1968; van Genuchten and Wierenga, 1976; Beven and Germann, 1981; Jarvis et al.1995). The second type of models are dual permeability models where Richards equation is applied to matrix and macropore regions separately with different hydraulic conductivities (Gerke and van Genuchten, 1993, 1996). The dynamic interaction between the two flow domains at any spatial location is established either based on the water contents of the two neighboring regions or on the hydraulic head difference between the two regions at the specific location (Simunek et al. 2003). As such, in order to quantify the flows between the matrix and the macropore regions at the scale of any spatial location in the subsurface it is necessary to determine either the water contents or the hydraulic heads at the two neighboring regions at the specified location. Using a three-dimensional dual porosity Darcy-Richards steady-state equation with the soil matrix and the macropores represented with different hydraulic conductivities and porosities, Nieber and Sidle (2010) were able to show vividly how the water table within a representative soil box in a hillslope evolves under different steady rain infiltration rates. By creating the macropores within the representative soil box as linear and ellipsoid tubes, filled with coarse material, and oriented at various directions, Nieber and Sidle (2010) were able to activate initially inactive macropores as the soil matrix was saturated from the bottom layer upwards under increasing rainfall infiltration rates, providing a viable conceptualization on how the matrix flows can interact dynamically with macropore flows along a hillslope under the gradually wetting conditions. They mention that their modeling results are consistent with the field experimental results of Sidle et al. (2000 and 2001).

While the multi-dimensional Darcy-Richards models were shown to simulate the SSSF over irregular bedrock geometry successfully at the scale of an individual hillslope (e.g. the successful unsaturated-saturated subsurface flow modeling study of Tromp-van Meerveld (2004) by means of HYDRUS-2D (Simunek et al.,

1999) over a heavily instrumented 48 m. long hillslope at Georgia, USA with well-delineated irregular bedrock topography), they require substantial numerical computations even over a single hillslope. Since there may be 10s of hillslopes over even a medium-size watershed (with drainage areas ~ 100 – 1000 sq km) it may be extremely difficult to model such a watershed's SSSF mechanism by means of multidimensional Darcy-Richards models for watershed hydrology simulations for a time range from a decade to a century (in the case of climate change impact assessments). Also, while they do have the mechanisms for interacting with macropore flows, the Darcy-Richards matrix flow models need to provide the water content/hydraulic head information at every spatial grid node for determining the interactions with the co-existing macropores along a hillslope subsurface at every time step of the model simulation. Furthermore, the multidimensional Darcy-Richards models, in their conventional forms, require information on the depth to the bedrock at fine grid resolution in order to be able to incorporate the bedrock surface geometry information into the model simulations at fine grid resolution over a hillslope. The bedrock surface geometry, which was shown to be a very important factor for SSSF, can at best be inferred for its macro trend behavior from the available digital elevation maps and digital soil survey databases such as SSURGO that provide limited information on the depth from the soil surface to bedrock at a number of locations over a hillslope.

The matrix flow component of SSSF may also be interpreted as a perched unconfined aquifer flow over a bedrock surface. The great hydraulic engineer Boussinesq (1877), assuming that such unconfined perched aquifer flow is essentially parallel to the underlying bedrock surface with a fixed slope along the flow domain, and using Dupuit's (1863) approximation, has developed the one-dimensional form of what is now known as the Boussinesq equation (Brutsaert, 2005). For the description of this saturated matrix flow, Boussinesq took the saturated thickness h, that is perpendicular to the underlying layer (bedrock surface layer), as the state variable, and formulated his equation along the bedrock surface layer direction x_1 (Please see Figure 1). The Boussinesq model was later used by Henderson and Wooding (1964) and Childs (1971). However, its derivation was clarified later by Brutsaert (2005).

Since it was shown by field studies (e.g. Sidle et al. 2001; Freer et al. 2002) that the bedrock surface geometry plays a fundamental role in determining SSSF characteristics, it was explicitly incorporated into several one-dimensional storage-type Boussinesq models. First, a one-dimensional storage-type Boussinesq model with kinematic wave approximation was introduced by Fan and Bras (1998) where the bedrock surface geometry longitudinal profile was described by a second order polynomial while the spatial variation of the hillslope width was quantified by means of the available topographic information. This study was followed by another one-dimensional storage-type Boussinesq model with kinematic wave approximation by Troch et al. (2002) who used a power-type function for describing the curvature of the longitudinal profile of the bedrock surface. By formulating the Boussinesq equation by taking moisture storage as the state variable, both studies were able to reduce the three-dimensional geometry of a hillslope into one dimension. Both studies showed successful modeling results of runoff at hillslope scale. Later on, Troch et al. (2003) developed the formulation for the full storage-type one-dimensional Boussinesq model under uniform bedrock profile in the longitudinal direction while accounting for the variability of the hillslope width in the transverse direction. This 1D storage-type Boussinesq model of Troch et al. (2003) was extended further by Hilberts et al. (2004) in order to account for the effect of the longitudinal profile of the bedrock surface along a hillslope. However, in their formulation Hilberts et al. (2004) left the slope of the bedrock surface profile as an implicit function of the location along the hillslope. As such, if it were to be applied to a real hillslope for modeling the matrix flow component of the SSSF, it would require detailed information on the evolution of the profile slope with each spatial increment. In summary, the storage-type Boussinesq equations in one dimension along the bedrock surface profile of a hillslope have shown how the bedrock surface longitudinal profile can be incorporated into the matrix flow equations with successful simulation results when compared to 3D Darcy-Richards matrix flow model. While the one-dimensional formulations of the Boussinesq model have shown successful application results when modeling the matrix flow component, they will have problems in dynamically interacting with macropore flows along a hillslope since macropore flows occur in generally tubular channels in three dimensions. These one-dimensional models will also have problems in interacting with other flow processes, such as rill/gully flows, when modeling hydrologic flow processes at the scale of a watershed. Also, the bedrock surface has essentially a two-dimensional geometry, where not only the longitudinal profile along the hillslope but also the transverse profile perpendicular to the main hillslope direction influences the subsurface stormflow over the bedrock. Therefore, it is necessary to consider the two-dimensional form of the Boussinesq equation in order to accommodate the two-dimensional geometry of the bedrock surface and to be able to interact with other component flow processes. Brutsaert (2005) provided a two-dimensional (2D) formulation for the Boussinesq model for matrix flow over a uniformly sloping flat 2D impeding layer (bedrock surface) with a fixed downward slope in the main longitudinal flow direction along a hillslope, but flat (zero slope) along the transverse direction (please see Figure 1). Taking his coordinates x_1 and y respectively parallel and perpendicular to the uniformly sloped bedrock surface direction along a hillslope, Brutsaert (2005) formulated the 2D Boussinesq model for matrix flow for the saturated thickness η perpendicular to the bedrock surface (please see Figure 1) as

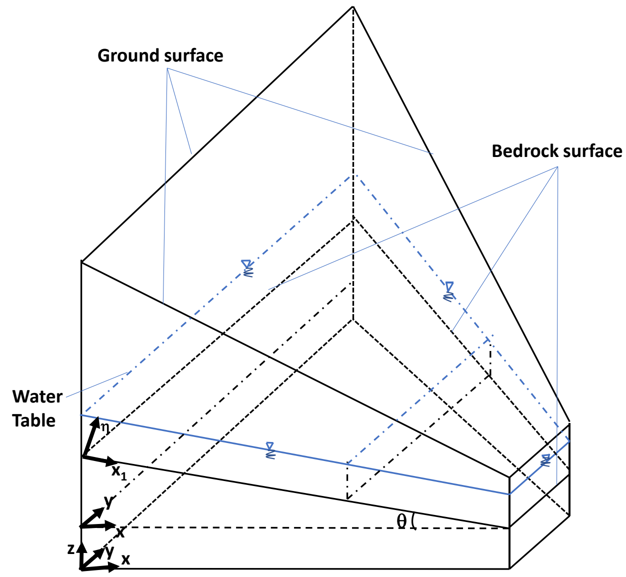

Figure 1. Matrix flow over a bedrock surface with a fixed downward slope in the longitudinal (hillslope) direction while having a flat transverse direction profile.

$$n_e \frac{\partial \eta}{\partial t} = Cos\theta K_s \frac{\partial}{\partial x_1}\left(\eta \frac{\partial \eta}{\partial x_1}\right) + Sin\theta K_s \frac{\partial \eta}{\partial x_1} + K_s \frac{\partial}{\partial y}\left(\eta \frac{\partial \eta}{\partial y}\right) + q_v \quad (1)$$

where θ is the fixed angle of the bedrock surface slope along the hillslope, n_e is the drainable porosity, K_s is constant saturated hydraulic conductivity and q_v is the recharge rate into the flow domain. Kavvas et al. (2004) also developed a 2D Boussinesq model for subsurface stormflow over a uniformly downward sloping impeding (infiltrating) layer along the hillslope direction but flat (zero slope) along the transverse direction as a component of their Watershed Environmental Hydrology (WEHY) model. However, since their subsurface stormflow model is just one component of various flow processes within their watershed model, they formulated the model with respect to a coordinate system that is common to all component hydrologic processes of the watershed. As such, they took the common horizontal x coordinate instead of the x_1 coordinate (which is along longitudinal bedrock surface direction) while using the same y coordinate in Brutsaert's (2005) 2D Boussinesq model (Equation (1)). Also, their state variable H is related to the saturated thickness η by

$$H = \eta\, Cos\theta \quad (2)$$

and based on the coordinates x and x_1,

$$\frac{\partial x}{\partial x_1} = Cos\theta \tag{3}$$

In the WEHY model the motion equations in the x and y directions were formulated as (Kavvas et al. 2004);

$$Q_x(x, y, t) = -H(x, y, t)Cos\theta K_s(x, y)\left(\frac{\partial H(x,y,t)}{\partial x} Cos\theta + Sin\theta\right) \tag{4}$$

$$Q_y(x, y, t) = -H(x, y, t)K_s(x, y)\left(\frac{\partial H(x,y,t)}{\partial y}\right) \tag{5}$$

respectively for the x-direction and y-direction flow discharges per unit width, using the Dupuit (1863) approximation within Boussinesq framework. The continuity equation for the SSSF component of the WEHY model was formulated as (Kavvas et al. 2004);

$$n_e \frac{\partial H(x,y,t)}{\partial t} = -\frac{\partial Q_x(x,y,t)}{\partial x} - \frac{\partial Q_y(x,y,t)}{\partial y} + q_v(x, y, t) \tag{6}$$

where $q_v(x, y, t)$ is the net vertical inflow/outflow rate into/from the SSSF domain. The vertical inflow (recharge) from the unsaturated soil zone into the SSSF zone is calculated in the WEHY model by the variably saturated rectangular profile approximation model (Chen et al. 1994a,b) that provides a comprehensive quantification of the vertical soil water flow above the saturated subsurface stormflow domain under both transient infiltration and evapotranspiration conditions while fully accounting for the spatial heterogeneity of the saturated hydraulic conductivity (Chen et al. 1994a,b). When the motion equations (4) and (5) of the SSSF component of WEHY model are combined with its SSSF continuity equation (6), the governing equation of 2D SSSF over an impeding layer with uniform downward slope in the hillslope direction but flat in the transverse direction is obtained as,

$$n_e \frac{\partial H(x,y,t)}{\partial t} = (Cos\theta)^2 \frac{\partial}{\partial x}\left(K_s(x, y)H(x, y, t)\frac{\partial H(x,y,t)}{\partial x}\right) + Sin\theta Cos\theta \frac{\partial}{\partial x}(K_s(x, y)H(x, y, t)) + \frac{\partial}{\partial y}\left(K_s(x, y)H(x, y, t)\frac{\partial H(x,y,t)}{\partial y}\right) + q_v(x, y, t) \tag{7}$$

After performing the transformations, specified by Equations (2) and (3), it can be shown that the governing equation (7) of 2D SSSF in WEHY model is equivalent to the 2D SSSF Equation (1) of Brutsaert (2005). WEHY model was successfully applied to various size watersheds in Japan (Chen et al. 2004a,b), Vietnam (Cuong et al. 2018), Malaysia (Amin et al. 2019), Thailand

(Wuthiwongyothin et al. 2015), Turkey (Gorguner et al. 2019), and California (Kavvas et al. 2006; Ohara et al. 2014; Trinh et al. 2017). However, since the WEHY model was developed in the late 1990s, the authors of the WEHY model were not aware of the field studies that reported the fundamental importance of bedrock surface geometry and its representative profile shapes in 2D. As such, in order to account for the impact of 2D bedrock surface geometry on SSSF, and to be able to dynamically couple the SSSF component with other hydrologic component processes within a watershed it is necessary to extend the existing 2D Boussinesq models for the 2D bedrock surfaces that are uniformly downward sloping in the main hillslope direction but flat in the transverse direction (Kavvas et al. 2004; Brutsaert, 2005) to various hillslope-scale 2D bedrock surface profiles that were reported in the above-mentioned field studies. Consequently, the main objective of this study is to develop the governing equations for 2D Boussinesq-type models of the matrix flow component of SSSF that will incorporate the explicit hillslope-scale 2D bedrock surface geometries while also accommodating the irregular shape of the hillslope in plan-view.

In the following, first the above-mentioned governing equations for 2D Boussinesq-type matrix flow component of SSSF shall be developed under various 2D bedrock surface geometries. Then, the developed equations will be used to numerically simulate matrix flows over various common 2D bedrock surface geometries in order to investigate the potential utility of the developed theory.

2. GOVERNING EQUATIONS OF 2D MATRIX FLOW COMPONENT OF SUBSURFACE STORMFLOW UNDER VARIOUS 2D BEDROCK SURFACE GEOMETRIES

While the above-mentioned 2D Boussinesq models are based on uniformly sloping bedrock surface profiles along a hillslope, the field observations of the bedrock surface geometry have shown that while the surface is irregular at small increments both along the hillslope and in the transverse direction to the hillslope,

hillslope-scale profile trends in the bedrock surface geometry can be identified. The hillslope-scale bedrock surface profile shapes may be approximately concave upwards both in the main hillslope direction (eg. Uchida et al. 2002; Kosugi et al. 2006) as well as in the transverse directions (eg. Noguchi et al. 1999; Torres et al. 1998), they may be approximately sinusoidal shaped in the hillslope direction (eg. Noguchi et al. 1999; Wienhofer and Zehe, 2014) or in both directions (eg. Sidle et al. 2000, 2001; Freer et al. 2002), or they may be partially concave and partially straight profiles along the hillslope direction (eg. Uchida et al. 2004). In the modeling of the SSSF process at the scale of a medium-size watershed, the information the modeler has is the digital elevation map of the watershed and depth to the bedrock at a limited number of locations from soil survey data. Therefore, from such information the modeler can reasonably infer hillslope-scale approximate shapes about the longitudinal and transverse profiles of the bedrock surface geometry. Consequently, in the following the 2D governing equations of matrix flow will be developed within the Boussinesq-Dupuit framework under various hillslope-scale bedrock surface profiles in two dimensions.

2.1. Case of Concave Upward Bedrock Surface Profile both in Longitudinal and Transverse Directions over a Variable-Width Hillslope:

Referring to Figure 2 which shows a bedrock surface with longitudinally and transverse-direction concave-upward profiles, tilting downward in the longitudinal hillslope direction, over a variable-width hillslope, the 2D governing equations of the matrix flow component of SSSF will be developed with the saturated thickness h(x,y,t) perpendicular to the bedrock surface at any location, as the state variable. The governing equations will be developed with respect to the Cartesian coordinate system (x,y,z) with x denoting the distance along the horizontal direction from the top of the hillslope toward its outlet, y denoting the horizontal distance along the transverse direction which is perpendicular to the x direction, and z representing the vertical distance upward from a reference location, shown in Figure 2. Since the SSSF is only one component among various hydrologic flow processes within a watershed it is convenient to take a common coordinate system for all component hydrologic processes within a watershed.

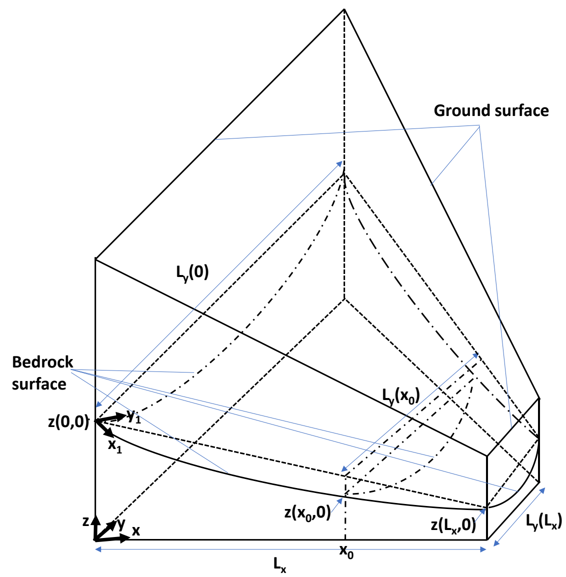

Figure 2. Bedrock surface geometry with longitudinally and transverse direction concave upward profiles along a variable-width hillslope (of arbitrary plan geometry).

Within the framework of the Cartesian coordinate system, described above, and referring to Figure 2, the hillslope-scale bedrock surface geometry z(x,y) with concave-upward profiles both in the longitudinal and transverse directions may be expressed as:

$$z(x,y) = (a - bx + cx^2) - \gamma L_y(x)y + \gamma y^2 \quad \text{where b>0, c>0, and } \gamma\text{>0} \qquad (8)$$

in order to account for the concavity of the bedrock surface in both longitudinal and transverse directions while also accounting for the hillslope width (L_y) variability along the hillslope, and ensuring that the bedrock concave-upward transverse profiles will have the same elevation both at the start and the end of any particular transverse-direction profile at any location x down the hillslope. Within the framework of Equation (8) the transverse bedrock profile will evolve along a hillslope.

Within the Boussinesq-Dupuit framework and referring to Figure 2, the motion equation for matrix flow along the x-direction may be expressed as;

$$Q_x(x,y,t) = -K_s(\underline{x})\left(\frac{\partial x}{\partial x_1}\right)^2 h(x,y,t)\frac{\partial h(x,y,t)}{\partial x} - K_s(\underline{x})h(x,y,t)\frac{\partial x}{\partial x_1}\frac{\partial z}{\partial x} \qquad (9)$$

in terms of the x-direction flow discharge Q_x per unit width. In the motion equation (9), $\underline{x}=(x,y,z)$,

$$\frac{\partial z}{\partial x} = -b + 2cx - \gamma y\frac{\partial L_y(x)}{\partial x} \qquad (10)$$

and

$$\frac{\partial x}{\partial x_1} = \frac{1}{\sqrt{1+\left(-b+2cx-\gamma y\frac{\partial L_y(x)}{\partial x}\right)^2}} \quad . \qquad (11)$$

Substituting expressions (10) and (11) into the motion equation (9) results in

$$Q_x(x,y,t) = -K_s(\underline{x})\frac{1}{1+\left(-b+2cx-\gamma y\frac{\partial L_y(x)}{\partial x}\right)^2}h(x,y,t)\frac{\partial h(x,y,t)}{\partial x} - K_s(\underline{x})h(x,y,t)\frac{-b+2cx-\gamma y\frac{\partial L_y(x)}{\partial x}}{\sqrt{1+\left(-b+2cx-\gamma y\frac{\partial L_y(x)}{\partial x}\right)^2}} \qquad (12)$$

as the explicit form of the motion equation in x-direction. Similarly, the y-direction motion equation in terms of the discharge Q_y per unit width may be obtained as

$$Q_y(x,y,t) = -K_s(\underline{x})\frac{1}{1+\left(-\gamma L_y(x)+2\gamma y\right)^2}h(x,y,t)\frac{\partial h(x,y,t)}{\partial y} - K_s(\underline{x})h(x,y,t)\frac{-\gamma L_y(x)+2\gamma y}{\sqrt{1+\left(-\gamma L_y(x)+2\gamma y\right)^2}} \qquad (13)$$

Recognizing from the recent field studies (Weiler et al. 2005) that the drainable porosity n_e varies with soil depth, the continuity equation for the matrix flow component of SSSF over a bedrock surface may be expressed as,

$$n_e(h)\frac{\partial h(x,y,t)}{\partial t} = -\frac{\partial Q_x(x,y,t)}{\partial x} - \frac{\partial Q_y(x,y,t)}{\partial y} + q_v(x,y,t) \qquad (14)$$

Combining the motion equations (12) and (13) with the continuity equation (14) results in

$$n_e(h)\frac{\partial h(x,y,t)}{\partial t} =$$

$$\frac{\partial}{\partial x}\left[K_s(\underline{x})\frac{1}{1+\left(-b+2cx-\gamma y\frac{\partial L_y(x)}{\partial x}\right)^2}h(x,y,t)\frac{\partial h(x,y,t)}{\partial x}+K_s(\underline{x})h(x,y,t)\frac{-b+2cx-\gamma y\frac{\partial L_y(x)}{\partial x}}{\sqrt{1+\left(-b+2cx-\gamma y\frac{\partial L_y(x)}{\partial x}\right)^2}}\right]+$$

$$\frac{\partial}{\partial y}\left[K_s(\underline{x})\frac{1}{1+(-\gamma L_y(x)+2\gamma y)^2}h(x,y,t)\frac{\partial h(x,y,t)}{\partial y}+K_s(\underline{x})h(x,y,t)\frac{-\gamma L_y(x)+2\gamma y}{\sqrt{1+(-\gamma L_y(x)+2\gamma y)^2}}\right]+$$

$$q_v(x,y,t) \tag{15}$$

as the governing equation of the 2D matrix flow component of SSSF in the soil matrix above a bedrock surface as an impeding layer with both longitudinal and transverse-direction concave-upward profiles at a variable-width hillslope at hillslope scale.

2.2. Case of Convex Upward Bedrock Surface Profile both in Longitudinal and Transverse Directions over a Variable-Width Hillslope:

Within the framework of the Cartesian coordinate system, described above, and referring to Figure 3, the hillslope-scale downward-tilting bedrock surface geometry z(x,y) with convex-upward profiles both in the longitudinal and transverse directions may be expressed again by Equation (8) with $b>0$, $c<0$ and $\gamma<0$. This surface geometry formulation again ensures equal bedrock surface elevation at both ends of a transverse-direction profile at any longitudinal location of the hillslope. Referring to Figure 3, for this bedrock surface as an impeding layer with both longitudinal and transverse-direction convex-upward profiles at a variable-width hillslope at hillslope scale, the governing equation for 2D matrix flow component of SSSF is again given by Equation (15) with the parameter values $b>0$, $c<0$ and $\gamma<0$.

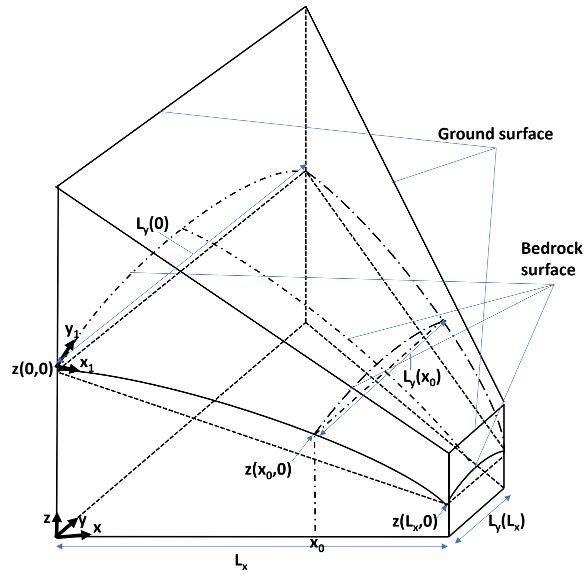

Figure 3. Bedrock surface geometry with longitudinal and transverse direction convex upward profiles along a variable-width hillslope (of arbitrary plan geometry).

2.3. Case of Concave Upward Bedrock Surface Profile in Longitudinal Direction but Flat Profile in the Transverse Direction:

In this case, as shown in Figure 4, the bedrock surface geometry with a longitudinally downward tilting concave-upward profile and flat transverse-direction profile may be expressed again by Equation (8) with parameters $b>0$, $c>0$ and $\gamma=0$. As such the governing equation for 2D matrix flow component of SSSF in the soil matrix above a bedrock surface as an impeding layer with a longitudinally concave-upward profile but with a flat transverse-direction profile at hillslope scale may be expressed again by Equation (15) with parameters $b>0$, $c>0$ and $\gamma=0$.

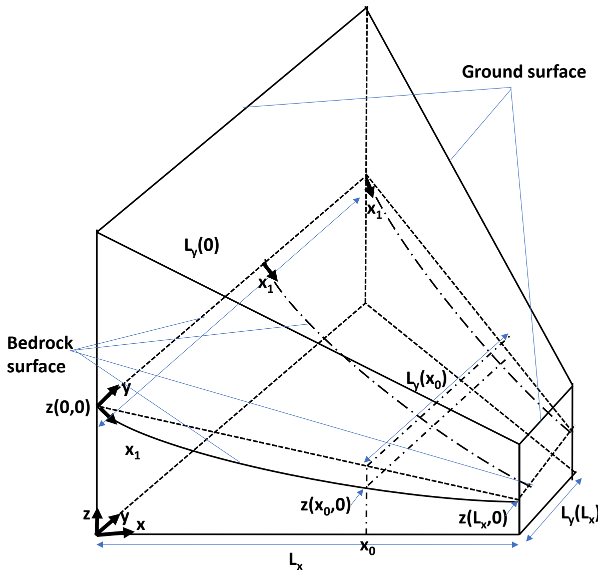

Figure 4. A bedrock surface geometry that has concave-upward profile in the longitudinal (hillslope) direction while being flat in the transverse y direction.

2.4. Case of Convex Upward Bedrock Surface Profile in Longitudinal Direction but Flat Profile in the Transverse Direction:

In this case, referring to Figure 5, the bedrock surface geometry with a longitudinally downward tilting convex-upward profile and flat transverse-direction profile may be expressed again by Equation (8) with parameters $b>0$, $c<0$ and $\gamma=0$.

As such, the governing equation of the 2D matrix flow component of SSSF in the soil matrix above a bedrock surface as an impeding layer with a longitudinally convex-upward profile but with a flat transverse-direction profile at hillslope scale may be expressed again by Equation (15) with parameters $b>0$, $c<0$ and $\gamma=0$.

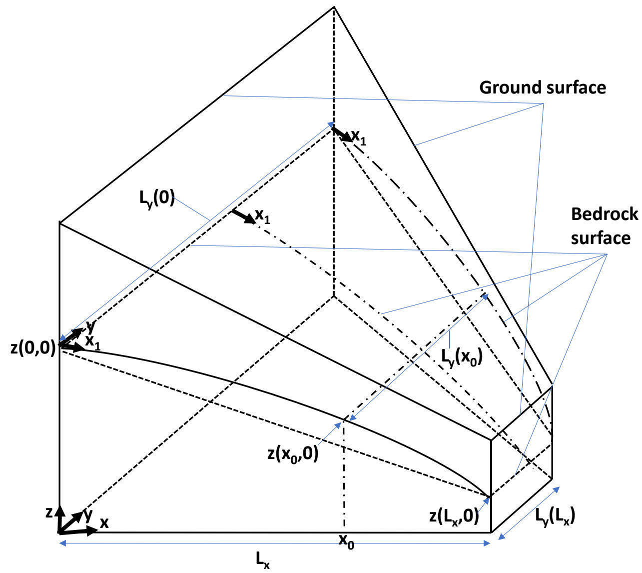

Figure 5. A Bedrock surface geometry that has convex-upward profile in the longitudinal (hillslope) direction while being flat in the transverse y direction.

2.5. Case of Partially Concave Upward and Partially Downward Straight-Sloping Bedrock Surface Profile in Longitudinal Direction but Being Flat in the Transverse Direction:

Motivated by the bedrock surface profiles, shown in Uchida et al (2004), and referring to Figure 6, the geometry of a partially concave upward and partially downward straight-sloping longitudinal profile of a bedrock surface with a flat profile in the transverse direction may be expressed as:

$$z(x,y) = (a - (\alpha + cx_0)x + cx^2) \quad \text{for} \quad 0 < x \leq x_0 \text{ where } c>0$$

$$= (a - \alpha x) \quad \text{for} \quad x_0 < x \leq L_x \text{ where } \alpha>0 \qquad (16)$$

which results in

$$\frac{\partial z}{\partial x} = -(\alpha + cx_0) + 2cx \quad \text{for} \quad 0 < x \leq x_0$$

$$= -\alpha \quad \text{for} \quad x_0 < x \leq L_x \qquad (17)$$

and

$$\frac{\partial x}{\partial x_1} = \frac{1}{\sqrt{1+(2cx-(\alpha+cx_0))^2}} \quad \text{for} \quad 0 < x \leq x_0$$

$$= \frac{1}{\sqrt{1+\alpha^2}} \quad \text{for} \quad x_0 < x \leq L_x \qquad (18)$$

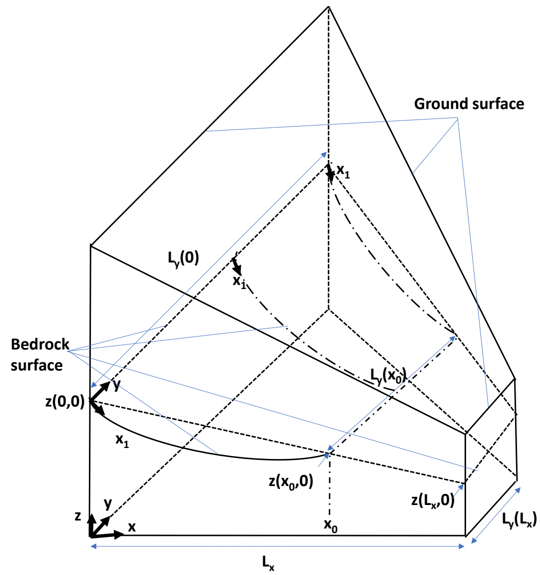

Figure 6. A bedrock surface with a concave-upward profile in the longitudinal (hillslope) direction in the interval (0, x_0), then straight with a fixed downward slope in the interval (x_0, L_x), while being flat in the transverse y direction.

Accordingly, the x-direction motion equation takes the form

$$Q_x(x,y,t) = -K_s(\underline{x})\frac{1}{1+(2cx-(\alpha+cx_0))^2}h(x,y,t)\frac{\partial h(x,y,t)}{\partial x} - K_s(\underline{x})h(x,y,t)\frac{2cx-(\alpha+cx_0)}{\sqrt{1+(2cx-(\alpha+cx_0))^2}} \quad . \quad \text{for} \quad 0 < x \le x_0 \quad (19)$$

and

$$Q_x(x,y,t) = -K_s(\underline{x})\frac{1}{1+\alpha^2}h(x,y,t)\frac{\partial h(x,y,t)}{\partial x} - K_s(\underline{x})h(x,y,t)\frac{-\alpha}{\sqrt{1+\alpha^2}} \quad \text{for } x_0 < x \le L_x \quad (20)$$

Since in the transverse y-direction

$$\frac{\partial z}{\partial y} = 0 \quad (21)$$

one obtains again equation (13) with γ=0 for the y-direction motion equation. Then substituting x and y-direction motion equations into the continuity equation (14) yields

$$n_e(h)\frac{\partial h(x,y,t)}{\partial t} =$$

$$\frac{\partial}{\partial x}\left[K_s(\underline{x})\frac{1}{1+\left(2cx-(\alpha+cx_0)\right)^2}h(x,y,t)\frac{\partial h(x,y,t)}{\partial x} + K_s(\underline{x})h(x,y,t)\frac{2cx-(\alpha+cx_0)}{\sqrt{1+\left(2cx-(\alpha+cx_0)\right)^2}}\right] +$$

$$\frac{\partial}{\partial y}\left[K_s(\underline{x})h(x,y,t)\frac{\partial h(x,y,t)}{\partial y}\right] + q_v(x,y,t) \qquad \text{for} \quad 0< x \le x_0 \; ; \; 0 \le y \le L_y(x) \quad (22)$$

and

$$n_e(h)\frac{\partial h(x,y,t)}{\partial t} = \frac{\partial}{\partial x}\left[K_s(\underline{x})\frac{1}{1+\alpha^2}h(x,y,t)\frac{\partial h(x,y,t)}{\partial x} + K_s(\underline{x})h(x,y,t)\frac{-\alpha}{\sqrt{1+\alpha^2}}\right] +$$

$$\frac{\partial}{\partial y}\left[K_s(\underline{x})h(x,y,t)\frac{\partial h(x,y,t)}{\partial y}\right] + q_v(x,y,t) \qquad \text{for } x_0 < x \le L_x \; ; \; 0 \le y \le L_y(x) \quad (23)$$

for the governing equation of matrix flow over a bedrock surface with a partially concave upward and partially straight downward sloping longitudinal profile but with a flat transverse direction profile.

2.6. Case of a Bedrock Surface with a Downward-sloping Sinusoidal Longitudinal Profile but with a Flat Transverse Direction Profile:

Referring to Figure 7, assuming the bedrock surface in the longitudinal direction can be expressed by a combination of harmonic functions with a fundamental period equal to the horizontal length L_x of the hillslope in the x-direction, one can define the fundamental frequency f_0 by

$$f_0 = \frac{1}{L_x} = \frac{1}{N\Delta x} \qquad (24)$$

where Δx is the sampling interval along x-direction and $N=L_x/\Delta x$ is the number of grids along the x-direction. Hence, any x-distance from the horizontal origin (corresponding to the top of the hillslope) may be expressed as

$$x = r\Delta x\,, \qquad 0 \le x \le L_x;\;\; 0 < r = x/\Delta x \le N \quad . \qquad (25)$$

Hence, the downward sloping (with a fixed slope) sinusoidal profile of the bedrock surface in the longitudinal direction, with grid increments Δx, may be approximated by the following harmonic representation:

$$z(x) \cong a - bx + A_0 + \sum_{j=1}^{\left|\frac{N}{2}\right|}\left[A_j Cos\left(\frac{2\pi jx}{L_x}\right) + B_j Sin\left(\frac{2\pi jx}{L_x}\right)\right] \qquad (26)$$

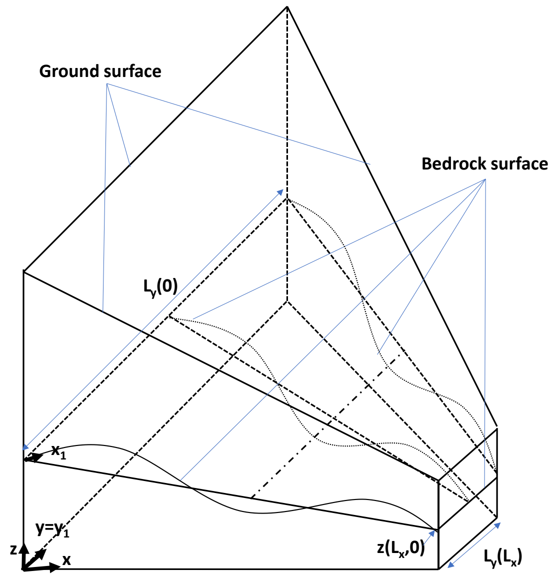

Figure 7. A bedrock surface with a downward sloping sinusoidal profile in the longitudinal direction, but flat in the transverse y direction.

in analogy to the representation of sinusoidal hydrologic time series (Salas et al. 1997) now recast into the ordered (from the top of the hillslope toward its bottom) spatial dimension in x-direction. In equation (26) $\left|\frac{N}{2}\right|$ is the integer part of N/2. Since the bedrock surface profile in the transverse direction y is taken to be flat, the 2D bedrock surface geometry may be approximated by;

$$z(x,y) = a - bx + A_0 + \sum_{j=1}^{\left|\frac{N}{2}\right|}\left[A_j Cos\left(\frac{2\pi jx}{L_x}\right) + B_j Sin\left(\frac{2\pi jx}{L_x}\right)\right] \tag{27}$$

where the harmonic coefficients A_j, j=0,1,2,..., $\left|\frac{N}{2}\right|$ and B_j , j=1,2,..., , $\left|\frac{N}{2}\right|$ may be estimated by

$$A_0 = \frac{1}{N}\sum_{r=1}^{N}[z(r\Delta x, y) - a + br\Delta x] \tag{28}$$

$$A_j = \frac{2}{N}\sum_{r=1}^{N}[z(r\Delta x, y) - a + br\Delta x]\, Cos\left(\frac{2\pi jr\Delta x}{N\Delta x}\right) \quad , \text{j}= 1,2,\ldots, \left|\frac{N}{2}\right| \tag{29}$$

$$B_j = \frac{2}{N}\sum_{r=1}^{N}[z(r\Delta x, y) - a + br\Delta x]\, Sin\left(\frac{2\pi jr\Delta x}{N\Delta x}\right) \quad , \text{j}= 1,2,\ldots, \left|\frac{N}{2}\right| \tag{30}$$

where j=1,2,..., $\left|\frac{N}{2}\right|$ are the frequencies that are all integer multiples of the fundamental frequency $f_0 = \frac{1}{L_x} = \frac{1}{N\Delta x}$.

It follows from equation (27) that

$$\frac{\partial z}{\partial x} = \left\{ -b + \sum_{j=1}^{\left|\frac{N}{2}\right|} \frac{2\pi j}{L_x} \left[-A_j Sin\left(\frac{2\pi j x}{L_x}\right) + B_j Cos\left(\frac{2\pi j x}{L_x}\right) \right] \right\} = \{\Xi\} \quad (31)$$

Hence,

$$\frac{\partial x}{\partial x_1} = \frac{1}{\sqrt{1+\{\Xi\}^2}} \quad . \quad (32)$$

Accordingly, the x-direction motion equation takes the form

$$Q_x(x,y,t) = -K_s(\underline{x}) \frac{1}{1+\{\Xi\}^2} h(x,y,t) \frac{\partial h(x,y,t)}{\partial x} - K_s(\underline{x}) h(x,y,t) \frac{\{\Xi\}}{\sqrt{1+\{\Xi\}^2}} \quad (33)$$

Since in the transverse y-direction

$$\frac{\partial z}{\partial y} = 0 \quad (34)$$

one obtains again equation (13) with γ=0 for the y-direction motion equation. Then substituting x and y-direction motion equations into the continuity equation (14) yields

$$n_e(h) \frac{\partial h(x,y,t)}{\partial t} = \frac{\partial}{\partial x}\left[K_s(\underline{x}) \frac{1}{1+\{\Xi\}^2} h(x,y,t) \frac{\partial h(x,y,t)}{\partial x} + K_s(\underline{x}) h(x,y,t) \frac{\{\Xi\}}{\sqrt{1+\{\Xi\}^2}} \right] + \frac{\partial}{\partial y}\left[K_s(\underline{x}) h(x,y,t) \frac{\partial h(x,y,t)}{\partial y} \right] + q_v(x,y,t) \quad (35)$$

for the governing equation of matrix flow over a bedrock surface with a downward-sloping sinusoidal longitudinal profile but with a flat transverse profile.

2.7. Case of a General Two-dimensional Bedrock Surface Geometry:

Referring to the complicated, two-dimensional bedrock surface geometry, as shown in Figure 2 of Freer et al. (2002), one can employ image processing techniques that were developed for expressing any multidimensional image, to approximate such a geometry. A very popular method that is used in image processing and reconstruction is the discrete cosine transform (DCT) which was introduced by Ahmed et al. (1974) and later extended to multiple dimensions (Makhoul, 1980; Wikipedia, 2022). DCT has also applications in interpolation, data compression, pattern recognition, and speech coding (Rao and Yip, 1990).

Consider a rectangular bedrock with a complicated surface geometry, as in the bedrock surface of Freer et al. (2002), which has length L_x in the horizontal direction x along the hillslope, and length L_y in the transverse direction y orthogonal to the x-direction. If the bedrock surface elevation (with respect to a common datum) is sampled at grid increments Δx in the x-direction and Δy in the y-direction, such discretization of the bedrock surface geometry would result in $N_x = L_x/\Delta x$ increments in the x-direction, and $N_y = L_y/\Delta y$ increments in the y-direction. As such, any two-dimensional (2D) bedrock surface geometry, sampled at $N_x \cdot N_y$ point locations, can be approximated by a two-dimensional discrete cosine transform (2D-DCT). If one designates the origin node by (x=0, y=0), then one can approximate the geometry of the 2D bedrock surface by means of the 2D-DCT (Makhoul, 1980; Wikipedia, 2022) by

$$z(x,y) \cong z(n_x\Delta x, n_y\Delta y) =$$

$$\frac{1}{\mathrm{N}_x\mathrm{N}_y}\sum_{k_x=0}^{\mathrm{N}_x-1}\sum_{k_y=0}^{\mathrm{N}_y-1} A(k_x,k_y)Cos\left[\frac{\pi(2n_x\Delta x+\Delta x)k_x}{2\mathrm{N}_x\Delta x}\right]Cos\left[\frac{\pi(2n_y\Delta y+\Delta y)k_y}{2\mathrm{N}_y\Delta y}\right] \quad (36)$$

$$\text{for } 0 \le n_x < \frac{L_x}{\Delta x} - 1 \ ; \ \ 0 \le n_y < \frac{L_y}{\Delta y} - 1; \text{ or } 0 \le n_x < \mathrm{N}_x - 1; \ 0 \le n_y < \mathrm{N}_y - 1 \ . \quad (37)$$

For approximating the complicated bedrock surface geometry by 2D-DCT, it is necessary to estimate the DCT coefficients $A(k_x,k_y)$. These coefficients may be estimated by means of the inverse 2D-DCT (Makhoul, 1980; Wikipedia, 2022) as:

$$\mathcal{A}(k_x,k_y) = 4\sum_{n_x=0}^{\mathrm{N}_x-1}\sum_{n_y=0}^{\mathrm{N}_y-1} z(n_x\Delta x, n_y\Delta y)Cos\left[\frac{\pi(2n_x\Delta x+\Delta x)k_x}{2\mathrm{N}_x\Delta x}\right]Cos\left[\frac{\pi(2n_y\Delta y+\Delta y)k_y}{2\mathrm{N}_y\Delta y}\right]$$

$$\text{for } 0 \le k_x < \mathrm{N}_x - 1; \ 0 \le k_y < \mathrm{N}_y - 1 \quad (38)$$

and then by the relationships (Makhoul, 1980),

$$A(k_x,k_y) = \mathcal{A}(k_x,k_y) \qquad \text{for } k_x \ne 0; \ \ k_y \ne 0$$

$$A(k_x,k_y) = \mathcal{A}(0,0)/4 \qquad \text{for } k_x = 0; \ \ k_y = 0$$

$$A(k_x,k_y) = \mathcal{A}(0,k_y)/2 \qquad \text{for } k_x = 0; \ \ k_y \ne 0$$

$$A(k_x,k_y) = \mathcal{A}(k_x,0)/2 \qquad \text{for } k_x \ne 0; \ \ k_y = 0 \quad (39)$$

Once the bedrock surface is approximated by 2D-DCT by means of Equations (36), (37), (38) and (39), then one can approximate the surface gradients in x and y directions by,

$$\frac{\partial z(x,y)}{\partial x} \cong \frac{\partial z(n_x,n_y)}{\partial n_x} =$$

$$-\frac{1}{\mathrm{N}_x\mathrm{N}_y}\sum_{k_x=0}^{\mathrm{N}_x-1}\sum_{k_y=0}^{\mathrm{N}_y-1} A(k_x,k_y)\frac{\pi k_x\Delta x}{\mathrm{N}_x\Delta x} Sin\left[\frac{\pi(2n_x\Delta x+\Delta x)k_x}{2\mathrm{N}_x\Delta x}\right] Cos\left[\frac{\pi(2n_y\Delta y+\Delta y)k_y}{2\mathrm{N}_y\Delta y}\right] = \{\mathcal{Z}_x\} \qquad (40)$$

and

$$\frac{\partial z(x,y)}{\partial y} \cong \frac{\partial z(n_x,n_y)}{\partial n_y} =$$

$$-\frac{1}{\mathrm{N}_x\mathrm{N}_y}\sum_{k_x=0}^{\mathrm{N}_x-1}\sum_{k_y=0}^{\mathrm{N}_y-1} A(k_x,k_y)\frac{\pi k_y\Delta y}{\mathrm{N}_y\Delta y} Cos\left[\frac{\pi(2n_x\Delta x+\Delta x)k_x}{2\mathrm{N}_x\Delta x}\right] Sin\left[\frac{\pi(2n_y\Delta y+\Delta y)k_y}{2\mathrm{N}_y\Delta y}\right] = \{\mathcal{Z}_y\} \qquad (41)$$

Taking the coordinate system along the 2D bedrock surface as (x_1,y_1), with respect to the general motion equation (9) in the x-direction,

$$\frac{\partial x}{\partial x_1} = \frac{1}{\sqrt{1+\{\mathcal{Z}_x\}^2}} \qquad (42)$$

which leads to the motion equation in the x-direction as

$$Q_x(x,y,t) = -K_s(\underline{x})\frac{1}{1+\{\mathcal{Z}_x\}^2}\, h(x,y,t)\frac{\partial h(x,y,t)}{\partial x} - K_s(\underline{x})h(x,y,t)\frac{\{\mathcal{Z}_x\}}{\sqrt{1+\{\mathcal{Z}_x\}^2}} \qquad (43)$$

Similarly, in the y-direction,

$$\frac{\partial y}{\partial y_1} = \frac{1}{\sqrt{1+\{\mathcal{Z}_y\}^2}} \qquad (44)$$

which leads to the motion equation in the y-direction as

$$Q_y(x,y,t) = -K_s(\underline{x})\frac{1}{1+\{\mathcal{Z}_y\}^2}\, h(x,y,t)\frac{\partial h(x,y,t)}{\partial x} - K_s(\underline{x})h(x,y,t)\frac{\{\mathcal{Z}_y\}}{\sqrt{1+\{\mathcal{Z}_y\}^2}} \qquad (45)$$

Combining x-direction and y-direction motion equations with the continuity equation (14) results in

$$n_e(h)\frac{\partial h(x,y,t)}{\partial t} = \frac{\partial}{\partial x}\left[K_s(\underline{x})\frac{1}{1+\{\mathcal{Z}_x\}^2}h(x,y,t)\frac{\partial h(x,y,t)}{\partial x} + K_s(\underline{x})h(x,y,t)\frac{\{\mathcal{Z}_x\}}{\sqrt{1+\{\mathcal{Z}_x\}^2}}\right] +$$

$$\frac{\partial}{\partial y}\left[K_s(\underline{x})\frac{1}{1+\{\mathcal{Z}_y\}^2}h(x,y,t)\frac{\partial h(x,y,t)}{\partial y} + K_s(\underline{x})h(x,y,t)\frac{\{\mathcal{Z}_y\}}{\sqrt{1+\{\mathcal{Z}_y\}^2}}\right] + q_v(x,y,t) \qquad (46)$$

as the governing equation of matrix flow over a bedrock surface with any complicated geometry.

3. NUMERICAL ASSESSMENT OF THE DEVELOPED THEORY

To illustrate the potential of the proposed matrix flow model, a hypothetical numerical experiment was performed. The initial saturated thickness is 0 everywhere and the vertical recharge and seepage capacity of the flow domain are 0.05m/day and 0.002m/day respectively, and the recharge lasts for 10 days. Seepage through the bedrock occurs only when there is enough water above the bedrock surface. The length of the domain L is 200m and the width B is 50m. The hydraulic conductivity is 1 m/day and the drainage porosity is 0.4. The simulation duration T is 300 days. Two flow domains that have different bedrock surface geometry profiles were used (Figure 8). Geometries in Figures 8a and 8b show two cases: one that is concave in both the longitudinal (x) and transverse (y) directions, and the second that is flat in both directions, respectively. The two upstream boundary corner locations of the two geometries in Figure 8 have the same elevation. Similarly, the downstream corner locations of the two geometries have the same elevation. No-flow boundary conditions are applied at the upstream and lateral boundaries. At the downstream, water flows parallel to the bedrock surface.

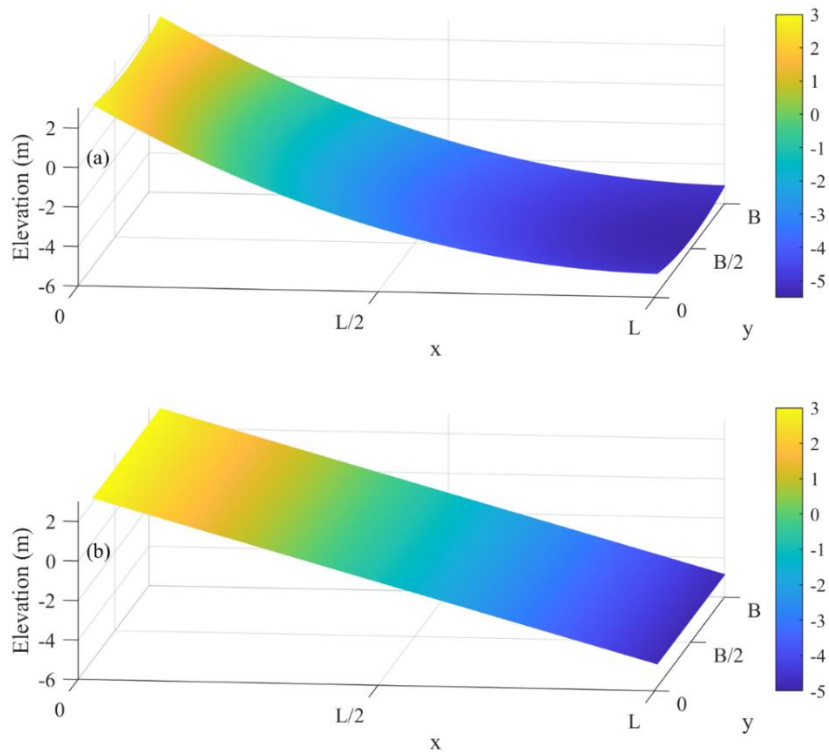

Figure 8. Two underlying bedrock surface geometries in the numerical experiment: (a) concave upward in both x and y directions; (b) flat in both x and y directions. The two upstream corners and the two downstream corners of the respective geometries are at the same elevations.

The concavity of the geometry clearly affects the flow dynamics as shown in Figure 9. Figure 9 shows the saturated thickness at the downstream boundary through time under the two different geometry profiles. Figure 9a shows the saturated thickness increases at a similar speed initially in both geometries while the recharge occurs, but a larger maximum thickness that is above 1m (>20% increase) happens when the underlying bedrock surface is concave in both directions, when compared with that under the flat bedrock profile, because of the concavity of the underlying geometry. The time for water drainage in the system also varies under different bedrock profiles. The saturated thickness drops to zero earlier in the flat case than that in the concave case (Figure 9a). The saturated thickness along the transverse direction above the concave bedrock surface, shown in Figure 9b, also varies by location. The middle cross-section (i.e., $y=B/2$) for the concave bedrock profile has the largest saturated thickness corresponding to the lowest bedrock elevation (see Figure 8), and also reaches its maximum at a later time compared with those of the other transverse locations in Figure 9b. The saturated thickness reduces to zero at different times along the transverse locations of the downstream cross-section under the numerical settings (Figure 9b).

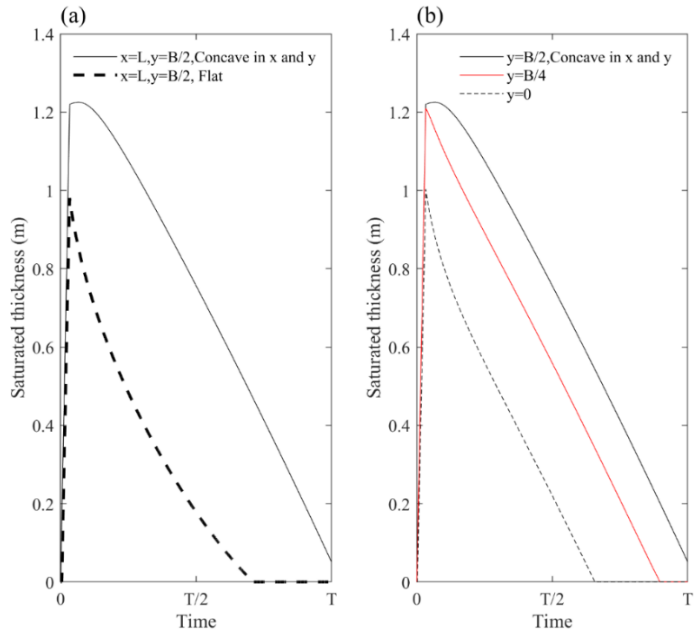

Figure 9. (a) Saturated thickness at the middle points of the downstream boundary (x=L, y=B/2) through time under two bedrock surface profiles; (b) Saturated thickness at three transverse locations at downstream boundary (x=L) through time under concave bedrock surface geometry that is concave in both directions. T is the total simulation time.

The saturated thickness variation from upstream to downstream at four different times under two bedrock geometries are shown in Figures 10(a-d). The saturated thickness on the bedrock that has concavity in both x and y directions is larger and does not reduce to 0 at the end of the simulation, while it drops to 0 in the flat case. In the flat case, the saturated thickness drops when approaching the downstream boundary due to the boundary condition where water flows out parallel to the bedrock surface (the gradients of bedrock elevation surface are different in the concave and flat cases at the downstream boundary). The variation of saturated thickness in the transverse direction under concave bedrock geometry that is concave in both x and y directions is shown in Figures 10 (e-f). The saturated thickness decreases as the flow location moves away from the middle section toward the lateral boundary, due to the concavity. The results in Figures 9 and 10 highlight the impact of the bedrock surface geometry on flow dynamics. From these results it may also be inferred that the proposed matrix flow model may be potentially useful in capturing such impact.

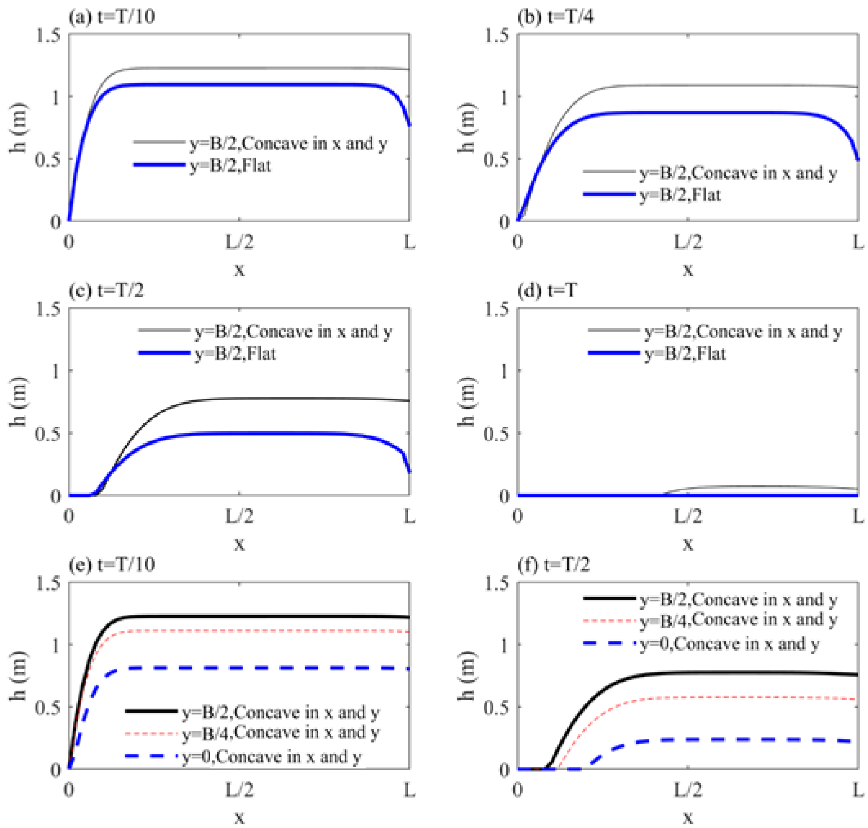

Figure 10. Saturated thickness, h, at the middle points ($y=B/2$) along the longitudinal direction x from upstream to downstream through time under two bedrock surface profiles at time $t=T/10$ (a); $t=T/4$ (b); $t=T/2$ (c); and $t=T$ (d); respectively; and saturated thickness at three transverse locations ($y=B/2$, $B/4$, 0) along the longitudinal direction from upstream to downstream under concave in x and y directions case at time $t=T/10$ (e) and $t=T/2$ (f) respectively. T is the total simulation time.

4. SUMMARY AND CONCLUSIONS

Various field studies have shown the fundamental influence of the bedrock surface geometry on subsurface stormflow (SSSF). Various field studies have also shown that the SSSF process consists of at least two major components: the matrix flow component and the macropore flow component that are in dynamic interaction toward forming the SSSF. This study focuses on the matrix flow component of SSSF. Furthermore, field studies have shown that the bedrock surface that underlies the SSSF has essentially a two-dimensional geometry, where not only the longitudinal profile along the hillslope but also the transverse profile perpendicular to the main hillslope direction influence the subsurface stormflow over the bedrock. Furthermore, the macropore flow itself being a multidimensional flow process, the general setting for the dynamic interaction of the matrix flow and macropore flow components of SSSF is the treatment of both of these processes as multidimensional flow processes. Within this framework, this study attempted to extend the existing 2D Boussinesq model for the matrix component of SSSF that was developed for a 2D bedrock surface that slopes with a constant slope in the hillslope longitudinal direction but flat in the transverse direction, to various other bedrock surface geometries that were reported in field studies.

After the development of 2D Boussinesq models of SSSF matrix flow component for various 2D bedrock surface geometries in terms of their governing equations, the impacts of the two bedrock surface geometries on the SSSF matrix flow component were assessed by a numerical experiment where matrix flow over a concave upward surface in both longitudinal and transverse directions was compared against a flat surface. In both bedrock surface geometries, the matrix flow component of SSSF was simulated under the same initial and boundary conditions over a hillslope where the hillslope has the same horizontal x-direction and same transverse y-direction lengths. The basic difference among the two studied cases is the geometry of the bedrock surface. The results of this numerical assessment show how the 2D bedrock surface geometry impacts the 2D flow characteristics of the matrix flow. As may be seen from the figures of the numerical experiment, the matrix flow component of SSSF is clearly a 2D flow process that is highly impacted by the particular bedrock surface geometry.

5. REFERENCES

Ahmed, N, T. Natarajan, K.R. Rao, (1974), Discrete Cosine Transform", IEEE Transactions on Computers, C-23 (1): 90-93.

Amin, Z., A. Ercan, K. Ishida, Z.Q. Chen, S.Y. Jang, M.L. Kavvas (2019), “Impacts of Climate Change on the Hydro-Climate of Peninsular Malaysia”, Water,11(9):1798, DOI: 10.3390/w11091798.

Beven, K.J. (1981), “Kinematic subsurface stormflow”, Water Resour. Res., 17(5), 1419-1424.

Beven, K.J., and P.F. Germann (1982), “Macropores and water flow in soils”, Water Resour. Res., 18(5), 1311-1325.

Beven, K. and P. Germann, (2013), “Macropores and water flow in soils: revisited”, Water Resour. Res. VOL. 49,3071-3092, doi:10.1002/wrcr.20156

Boussinesq, J. (1877), Essai sur la theorie des eaux courantes, Mem. Acad. Sci. Inst. Fr., 23(1), 252–260.

Brutsaert, W. (2005), Hydrology: An Introduction, 605 pp., Cambridge Univ. Press, New York.

Chen, Z.Q., R.S. Govindaraju and M.L. Kavvas, (1994a), " Spatial averaging of unsaturated flow equations for areally heterogeneous fields: Development of models", Water Resour. Res., 30(2), 523-533.

Chen, Z.Q., R.S. Govindaraju and M.L. Kavvas, (1994b), " Spatial averaging of unsaturated flow equations for areally heterogeneous fields: Numerical simulations", Water Resour. Res., 30(2), 534-544.

Chen, Z.Q., M.L. Kavvas, J.Y. Yoon, C. Dogrul, K. Fukami, J. Yoshitani, T. Matsuura, (2004a), “Geomorphologic and soil hydraulic parameters for watershed environmental hydrology (WEHY) model”, Journal of Hydrologic Engineering, Vol.9, No.6, 465-489.

Chen, Z.Q., M.L. Kavvas, K. Fukami, J. Yoshitani, T. Matsuura, (2004b), “Watershed environmental hydrology (WEHY) model: Model Application”, Journal of Hydrologic Engineering, Vol.9, No.6, 480-490.

Chifflard, P., R. Kirnbauer, H. Zepp, N. Tilch, J. Didszun, B. Zillgens, S... Uhlenbrook, (2010), “Tracing runoff generation processes through different spatial scales in low and high mountain ranges”, IAHS Publication 336, 90-95.

Childs, E. C. (1971), Drainage of groundwater resting on a sloping aquifer, Water Resour. Res., 7(5), 1256–1263.

Cuong,H.V., A. Ercan, T. Nguyen, A. Nguyen, V. Nguyen, M.L. Kavvas, “Assessment of atmospheric conditions over the Hong Thai Binh river watershed by means of dynamically-downscaled ERA-20C reanalysis data”, Journal of Water and Climate Change, DOI: 10.2166/wcc.2018.291, 2018.

Dunne, T. and R.D. Black, (1970a), " An experimental investigation of runoff production in permeable soils", Water Resour. Res. 6, 478-90.

Dunne, T. and R.D.Black, (1970b), " Partial area contributions to storm runoff in a small New England watershed ", Water Resour. Res., 6, 1296-1311.

Dunne, T., (1978)," Field studies of hillslope flow processes", in *Hillslope Hydrology*, ed. by M.J.Kirkby.

Dupuit, J. (1863), Etudes theoriques et practiques sur le mouvement des eaux dans les canaux decouverts et a travers les terrains permeables, 2nd ed., Dunod, Paris

Fan, Y., and R. L. Bras (1998), Analytical solutions to hillslope subsurface storm flow and saturation overland flow, Water Resour. Res., 34(4), 921– 927.

Freer, J., J. McDonnell, K.J. Beven, N.E. Peters, D. Burns, R.P. Hooper, B. Aulenbach, and C. Kendal, (2002), “The role of bedrock topography on subsurface stormflow”, Water Resour. Res., 38(12).

Freeze RA. (1972a), “Role of subsurface flow in generating surface runoff: 1. Base flow contributions to channel flow”, Water Resources Research 8: 609–623.

Freeze A.R. (1972b), "Role of subsurface flow in generating surface runoff. 2.Upstream source areas", Water Resources Research, 8(5), 1272–1283.

Gerke, H.H., and M.Th. van Genuchten, (1993), "A dual-porosity model for simulating the preferential movement of water and solutes in structured porous media", Water Resour. Res., 29, 305-319.

Gerke, H.H., and M.Th. van Genuchten, (1996), "Macroscopic representation of structural geometry for simulating water and solute movement in dual-porosity media", Advances in Water Resources, Vol. 19, No. 6, pp. 343-357.

Gerke, H.H. (2006), "Preferential flow description for structured soils", J. Plant Nutr. Soil Sci., 169, 382-400.

Gorguner, M., M.L. Kavvas, K. Ishida, "Assessing the impacts of future climate change on the hydroclimatology of the Gediz Basin in Turkey by using dynamically downscaled CMIP5 projections", Science of the Total Environment 648, 481–499, 2019.

Guo, L., H. Lin, Bihang Fan, J. Nyquist, L. Toran, G. J. Mount. (2019), "Preferential flow through shallow fractured bedrock and a 3D fill-and-spill model of hillslope subsurface hydrology", Journal of Hydrology 576, 430–442.

Henderson, F. M., and R. A. Wooding, (1964), "Overland flow and groundwater flow from a steady rainfall of finite duration", J. Geophys. Res., 69(8), 1531-1540.

Hewlett, J.D. and A.R. Hibbert, (1967), " Factors affecting the response of small watersheds to precipitation in humid areas", in International Symposium on forest Hydrology, ed. by Sopper,W.E. and H.W.Lull, Pergamon Press, NY,275-90.

Hilberts, A. G. J., E. E. van Loon, P. A. Troch, and C. Paniconi (2004), The hillslope-storage Boussinesq model for non-constant bedrock slope, J. Hydrol., 291, 160–173, doi: 10.1016/j.jhydrol.2003.12.043.

Ho, C., T. Trinh, A. Nguyen, Q. Nguyen, A. Ercan, M.L. Kavvas, "Reconstruction and evaluation of changes in hydrologic conditions over a transboundary region by a regional climate model coupled with a physically-based hydrology model: Application to Thao river watershed", Science of the Total Environment, Volume 668, 768-779, 2019.

Jarvis, N.J., M. Larsson, P. Fogg, and A.D. Carter. (1995), "Validation of the dual-porosity model 'MACRO' for assessing pesticide fate and mobility in soils", 161–170. In A. Walker et al. (ed.) Pesticide movement to water. BCPC Monograph. 62. The British Crop Protection Council, Farnham, Surrey, UK.

Jones J.A.A. (1981), "The Nature of Soil Piping: a Review of Research", British Geomorphological Research Group Monograph Series(3).

Jones, J.A. A., (2010), "Soil piping and catchment response", Hydrol. Pro-cess., 24, 1548-1566.

Kavvas, M.L., Z.Q.Chen, C.Dogrul, J.Y.Yoon, N.Ohara, L.Liang, H.Aksoy, M.L.Anderson, J.Yoshitani, K.Fukami, T.Matsuura, (2004),"Watershed environmental hydrology (WEHY) model, based on upscaled conservation equations: Hydrologic module", Journal of Hydrologic Engineering, Vol.9, No.6, 450-464.

Kavvas, M.L., J. Yoon, Z.Q. Chen, L. Liang, E.C. Dogrul, N.Ohara, H. Aksoy, M.L. Anderson, J. Reuter, S. Hackley, (2006), “Watershed environmental hydrology model: Environmental module and its application to a California watershed”, Journal of Hydrologic Engineering, Vol.11, No.3, 261-272.

Kavvas M. L., T. Tu, A. Ercan and J. Polsinelli, (2020), “Fractional governing equations of transient groundwater flow in unconfined aquifers with multi-fractional dimensions in fractional time”, Earth Syst. Dynam., Vol. 11, 1–12; https://doi.org/10.5194/esd-11-1-2020

Keim, R.F., H.J. Tromp-van Meerveld, J.J. McDonnell, (2006), “A virtual experiment on the effects of evaporation and intensity smoothing by canopy interception on subsurface stormflow generation”, Journal of Hydrology, 327, 352-364.

Kohne, J. M., Kohne, S., & Simunek, J. (2009), “A review of model applications for structured soils: A water flow and tracer transport”, 104(1-4), 4- 35.

Kosugi, K., Katsura, S., Katsuyama, M., Mizuyama, T., (2006), “Water flow processes in weathered granitic bedrock and their effects on runoff generation in a small headwater catchment”, Water Resour. Res. 42 (2).

Loague, K. and J.E. VanderKwaak, (2002), “Simulating hydrological response for the R-5 catchment: comparison of two models and the impact of the roads”, Hydrol. Process. 16, 1015–1032.

Makhoul, J. (1980), "A fast cosine transform in one and two dimensions", IEEE Transactions on Acoustics, Speech, and Signal Processing. 28 (1): 27-34.

Martini, E., U. Wollschlager, S. Ogler, T. Behrens, P. Dietrich, F. Reinstorf, S. Zacharias, (2015), “Spatial and temporal dynamics of hillslope-scale soil moisture patterns: Characteristic states and transition mechanisms”, https://doi.org/10.2136/vzj2014.10.0150.

McDonnell J.J. (1990), “A rationale for old water discharge through macropores in a steep, humid catchment”, Water Resources Research 26:2821–2832.

McDonnell, J.J., Freer, J.E., Hooper, R.P., Kendall, C., Burns, D.A., Beven, K.J., Peters, N.E., (1996), “New method developed for studying flow in hillslopes”, Eos 77, 465-472.

McKnight, D. M., M.A. Burns, H. Barnard, R.S. Gabor, (2015), “Transport of dissolved organic matter from the hillslope to the stream: Using fluorescence spectroscopy to identify changing sources during snowmelt”, 17, EGU2015-EGU5219.

Mosley MP. (1979), “Streamflow generation in a forested catchment”, Water Resources Research 15: 795–806.

Mueller, M. H., A. Alaoui, C. Kuells, H. Leistert, K. Meusburger, C. Stumpp, C. Alewell, (2014), “Tracking water pathways in steep hillslopes by d180 depth profiles of soil water”, J. Hydrol., 519, 340- 352.

Nieber, J.L. and R.C. Sidle, (2010), “How do disconnected macropores in sloping soils facilitate preferential flow?”, Hydrol. Process. 24, 1582–1594.

Noguchi S, Tsuboyama Y, Sidle RC, Hosoda I. (1997), “Spatially distributed morphological characteristics of macropores in forest soils of Hitachi Ohta Experimental Watershed, Japan”, Journal of Forest Research 2: 207–215.

Noguchi S, Tsuboyama Y, Sidle RC, Hosoda I. (1999), “Morphological characteristics of macropores and the distribution of preferential flow pathways in a forested slope segment”, Soil Science Society of America Journal 63: 1413–1423.

Ohara, N., M.L. Kavvas, Z.Q. Chen, L. Liang, M. Anderson, J. Wilcox, and L. Mink, (2014), “Modelling atmospheric and hydrologic processes for assessment of meadow restoration impact on flow and sediment in a sparsely gauged California watershed”, Hydrological Processes, 28(7), 3053-3066.

Phillip, J.R., (1968), “The theory of absorption in aggregated media”, Aust. J. Soil Res. 6, 1-19.

Ragan, R.M., (1968), "An experimental investigation of partial area contribution", Proc. Gen. Assembly, Berne, IAHS,publ. 76, 241-249.

Rao, K.R. and Yip P. (1990), “Discrete Cosine Transform: Algorithms, Advantages, Applications”, Academic Press Professional, Inc. San Diego, USA. ISBN:978-0-12-580203-1.

Salas, J.D., J.W. Delleur, V. Yevjevich and W.L. Lane, (1997), Applied Modeling of Hydrologic Time Series, Water Resources Publications, 4th Ed.

Sidle R.C., Tsuboyama Y, Noguchi S, Hosoda I, Fujieda M, Shimizu T. (1995), “Seasonal hydrologic response at various spatial scales in a small forested catchment, Hitachi Ohta, Japan”, Journal of Hydrology 168: 227–250.

Sidle R.C., Tsuboyama Y, Noguchi S, Hosoda I, Fujieda M, Shimizu T. (2000), “Stormflow generation in steep forested headwaters: a linked hydrogeomorphic paradigm”, Hydrological Processes 14: 369–385.

Sidle RC, Noguchi S, Tsuboyama Y, Laursen K. (2001), “A conceptual model of preferential flow systems in forested hillslopes: evidence of self-organization”, Hydrological Processes 15: 1675–1692.

Simunek, J., Sejna, M., van Genuchten, M.Th., (1999), “The Hydrus-2D software package for simulating two-dimensional movement of water, heat and multiple solutes in variably saturated media. Version 2.0”, IGWMC-TPS-53, International Groundwater Modeling Center, Colorado School of Mines, Golden, Colorado.

Simunek, J., N.J. Jarvis, M.T. van Genuchten, and A. Gardends, (2003), “Review and comparison of models describing non-equilibrium and preferential flow and transport in the vadose zone”, J Hydrol, 272, 14-35.

Sloan, P.G. and I.D. Moore, (1984), “Modeling subsurface stormflow on steeply sloping forested watersheds”, Water Resour. Res. 20(12), 1815-1822.

Tani M. (1997), “Runoff generation processes estimated from hydrological observations on a steep forested hillslope with a thin soil layer”, Journal of Hydrology 200: 84–109.

Torres R, Dietrich WE, Montgomery DR, Anderson SP, Loague K. (1998), “Unsaturated zone processes and the hydrologic response of a steep, unchanneled catchment”, Water Resources Research 34: 1865–1879.

Trinh, T., K.Ishida, M.L. Kavvas, A. Ercan, K. Carr, (2017), "Assessment of 21st century drought conditions at Shasta Dam based on dynamically projected water supply conditions by a regional climate model coupled with a physically-based hydrology model", Science of the Total Environment, doi: 10.1016/j.scitotenv.2017.01.202; 586, 197-205.

Troch, P., E. van Loon, and A. Hilberts (2002), Analytical solutions to a hillslope-storage kinematic wave equation for subsurface flow, Adv. Water Resour., 25, 637–649, doi :10.1016/S0309–1708(02)00017-9.

Troch, P. A., C. Paniconi, and E. E. van Loon (2003), Hillslope-storage Boussinesq model for subsurface flow and variable source areas along complex hillslopes: 1. Formulation and characteristic response, Water Resour. Res., 39(11), 1316, doi: 10.1029/2002WR001728.

Troch PA, Berne A, Bogaart P, Harman C, Hilberts AGJ, Lyon SW, Paniconi C, Pauwels VRN, Rupp DE, Selker JS, Teuling AJ, Uijlenhoet R, Verhoest NEC, (2013), "The importance of hydraulic groundwater theory in catchment hydrology: the legacy of Wilfried Brutsaert and Jean-Yves Parlange", Water Resour Res 49:5099–5116.

Tromp-van Meerveld H.J. (2004), "Hillslope Hydrology: from Patterns to Processes", Ph.D. dissertation, Oregon State University, Corvallis, 270pp.

Tsuboyama Y, Sidle RC, Noguchi S, Hosoda I. (1994), "Flow and solute transport through the soil matrix and macropores of a hillslope segment", Water Resources Research 30: 879–890.

Uchida T., Kosugi K.i. and Mizuyama T. (2002), "Effects of pipe flow and bedrock groundwater on runoff generation in a steep headwater catchment in Ashiu, central Japan", Water Resources Research, 38(7).

Uchida T, Asano Y, Mizuyama T, McDonnell JJ. (2004), "Role of upslope soil pore pressure on lateral subsurface storm flow dynamics", Water Resources Research 40: W12401.

Uchida T. and Y. Asano, (2010), "Spatial variability in the flowpath of hillslope runoff and streamflow in a meso-scale catchment", Hydrol. Process. 24, 2277–2286.

van Genuchten, M. T. and P.J. Wierenga, (1976), "Mass transfer studies in sorbing porous media. I. Analytical Solutions", Soil Sci. Soc. Am. J., 40, 473-480.

Weiler, M., McDonnell, J.J., Tromp van Meerveld, I., Uchida, T., (2005), "Subsurface stormflow runoff generation processes", In: *Anderson, M.G. (Ed.), Encyclopedia of Hydrological Sciences*. John Wiley & Sons, Inc.

Weiler, M. and J.J. McDonnell, (2006), "Testing nutrient flushing hypotheses at the hillslope scale: a virtual experiment approach", J. Hydrol. 319, 339-356.

Weyman DR. (1973), "Measurement of the downslope flow in a soil", Journal of Hydrology 20: 267–288.

Whipkey, R.Z., (1965), " Subsurface stormflow from forested slopes", Intl.Assoc. Sci. Hydrol. Bull. 10, 74-85.

Wienhofer, J., & Zehe, E. (2014), "Predicting subsurface stormflow response of a forested hillslope—The role of connected flow paths",18, 121- 138.

Wikipedia, (2022), "Discrete Cosine Transform", Retrieved from https://en.wikipedia.org/w/index.php?title=Discrete cosine transform&oldid=963888909 (Accessed on January 11, 2022).

Woods, R., Rowe, L., (1996), "The changing spatial variability of subsurface flow across a hillside", Journal of Hydrology (New Zealand) 35, 49–84.

Wuthiwongyothin, S., S. Jang; K.Ishida and M.L. Kavvas, "Hydrologic Impact Assessment by a Physically-Based Hydro-Climate Model of Regional Climate Change for the Water Resources of the Upper Ping River Basin of Thailand", Proceedings of World Environmental and Water Resources Congress 2015: Floods, Droughts, and Ecosystems, pp. 1026-1030, May 2015.